Received 11 December 2025, accepted 03 July 2026, date of publication 30 September 2026
www.computingonline.net / computing@computingonline.net

Print ISSN 1727-6209
Online ISSN 2312-5381
DOI 10.47839/ijc.25.3.4838

Method and Software for Multi-Parametric Choosing Algorithms of UAVs Placement and Routing in Hazardous Space

LEONID OSTAPENKO, VYACHESLAV KHARCHENKO
National Aerospace University "KhAI", Kharkiv, 61070, Ukraine
(E-mail: l.ostapenko@csn.khai.edu, v.kharchenko@csn.khai.edu)

Corresponding author: Leonid Ostapenko (e-mail: l.ostapenko@csn.khai.edu).

ABSTRACT This paper considers the tasks of choosing algorithms for placing unmanned aerial vehicles (UAVs) to support communications and route formation in a hazardous cyber-physical 3D space. UAV placement is interpreted as the selection of spatial coordinates for relay UAVs that form a communication chain between a data source and receiver, primarily in flying LiFi or free-space optical networks. The proposed adaptive method selects a routing or placement algorithm using several environment indicators: obstacle density, obstacle-shape complexity, dynamic changes, communication constraints, cyber-physical risk, and mission priority. The method combines environment analysis, multi-indicator assessment of A*, RRT*, and greedy search, route construction, relay UAV placement, and swarm-characteristic evaluation. A software implementation in Python/Panda3D supports scenario configuration, adaptive algorithm selection, metric logging, and experimental comparison. The reported procedure is reproducible because input scenarios, seeds, algorithm modes, and run-level measurements are fixed. A series of 100 runs confirmed correct adaptive selection and no degradation of controlled safety and communication characteristics in the tested static scenarios.

KEYWORDS unmanned aerial vehicle; UAV swarm; hazardous space; 3D routing; relay placement; cyber-physical impact; A*; RRT*; greedy search; multi-indicator algorithm selection

I. INTRODUCTION

The use of unmanned aerial vehicle (UAV) swarms in hazardous spaces requires methods that simultaneously support environment modelling, obstacle-avoidance routing, and communication organization [1, 2]. A closely related research direction concerns flying LiFi networks and path-finding algorithms for UAV placement in obstacle-ridden spaces [3, 4]. Under such conditions, motion and communication depend on wireless interaction conditions [5-7], routing features in flying ad hoc networks [8, 9], and the spatial placement of aircraft and relays [10-13].

A hazardous space is understood as a dynamic 3D environment with mechanical obstacles, physical impacts, and information-related, including cybernetic, factors [14, 15]. These factors can change route availability, degrade radio communication conditions, reduce UAV autonomy, or increase the probability of failure. Examples include destroyed industrial, transport, and energy facilities, as well as water or mixed environments with obstacles and hazardous zones.

In this work, placement does not mean selecting a base, duty, or launch site for the swarm. It means calculating intermediate 3D positions for relay UAVs along or near a data-transmission route. For optical wireless communication, these positions must ensure line-of-sight visibility between neighboring nodes; for a radio channel, the same logic can be used after replacing the line-of-sight model with an appropriate radio-coverage and allowable-loss model.

The main idea is that the routing or placement algorithm should not be fixed in advance as an immutable mission parameter. When the occupied obstacle volume is small, obstacles are static, and the mission priority is rapid generation of an admissible solution, a greedy search may be appropriate. When the operational space is represented by a regular grid or graph and obstacle boundaries are approximated sufficiently well by this discretization, A* is a natural choice. When obstacles have arbitrary, elongated, or fragmented shapes and the environment changes over time, sampling-based approaches, in particular RRT*, can provide greater flexibility. Therefore, this work proposes moving from fixed algorithm selection to adaptive selection based on explicitly defined environmental features.

The article is organized as follows. Section II analyses related works and formulates the research objectives. Section III presents the formal problem statement. Sections IV and V describe the proposed method and the software tool for algorithm selection, respectively. Section VI presents and analyses the experimental results. Sections VII and VIII discuss the main contributions, limitations, scientific and practical implications of the method, and directions for future research.

II. ANALYSIS OF PUBLICATIONS AND RESEARCH OBJECTIVE

Route construction in an environment with obstacles is a classical problem in robotics, autonomous systems, and computer engineering. The best-known approaches include graph-based shortest-path methods, heuristic methods, and sampling-based algorithms. Dijkstra's algorithm finds the shortest path in a graph with non-negative weights [16], but without a heuristic it can be too expensive for large spaces. A* supplements graph search with a heuristic function and remains one of the basic approaches to route planning in a discretized space [17]. Its advantage is a clear optimization nature, while its drawback is dependence on discretization quality, space dimensionality, and obstacle complexity.

For continuous spaces or spaces without a natural regular-grid representation, sampling-based algorithms are often used. In randomized dynamic planning, the rapidly-exploring random tree (RRT) is used as a basis for fast exploration of a configuration or phase space [18]. The practical development of this class of methods is associated with RRT-Connect [19], whereas its theoretical strengthening is associated with RRT* and asymptotic optimality [20]. Modern works on 3D UAV planning in cluttered environments and reviews of metaheuristic approaches show that route quality depends not only on length but also on energy constraints, environment representation, heuristics, and computational stability [21-25].

Greedy and local heuristic methods are used when decision speed is the priority. They can quickly build a route in a space with a small occupied-volume fraction and without frequent local bottlenecks, but they risk being trapped in local minima, especially in the presence of densely placed, elongated, or fragmented obstacles [25]. For UAV tasks this property is critical: a route obtained quickly may require a larger number of relays because of poor visibility geometry or passage through zones with degraded communication.

A separate research direction concerns UAV networks and flying ad hoc networks (FANETs). In FANET systems the network topology changes rapidly, which complicates routing between moving nodes [8, 9]. Channel quality depends on aircraft position, altitude, line of sight, interference, and motion mode [5-7]. For optical wireless LiFi or free-space optical (FSO) networks this dependence is even stricter, since a line-of-sight break between neighboring relays directly interrupts the communication chain [3, 4]. Under such conditions, routing in the geometric sense cannot be considered separately from the communication problem.

Relay placement also has its own specificity. For static networks, it is often reduced to optimal coverage, connected-graph construction, or minimization of the number of nodes under range constraints [10-13, 26]. However, for a UAV swarm in a hazardous space, relay positions must be not only communication-admissible but also geometrically reachable. In addition, UAVs have limited autonomy and can be exposed to physical impacts and cyberattack risks. Therefore, placement in this work is considered not as a separate static coverage task but as a stage connected with the constructed route and the current environment state.

In related research, methods for decision making with several criteria, including the analytic hierarchy process (AHP) and TOPSIS, are often used for formal comparison of alternatives [27-30]. Such approaches operate with optimality criteria and, in optimization problems, may analyze Pareto-optimal solutions. This review is used only for terminological separation. The method proposed in this article is not an MCDM procedure, does not construct a Pareto front, and does not prove optimality with respect to a set of criteria. It performs multi-indicator algorithm selection using normalized environmental and mission features.

The relevance of updating the bibliographic basis is caused by the fact that in 2022-2026 UAV research shifted rapidly from individual route algorithms to autonomous networks, 5G/B5G scenarios, machine learning for communications, energy-aware routing, and NOMA approaches for UAV networks. Modern reviews and applied studies show that UAV placement tasks require simultaneous consideration of connectivity, energy, mobility, interference, route selection, and channel-state adaptation [31-35]. Therefore, in the proposed method algorithm selection is not reduced only to route length but is linked to communication and risk characteristics of the mission.

The objective of the article is to develop and justify a method for selecting UAV placement algorithms to support communications or route formation in 3D space. The main formulation concerns a flying network with relay UAVs, where it is necessary to select the minimum sufficient number of aircraft and their coordinates so that line of sight, allowable communication range, position reachability, and acceptable risk are preserved between neighboring nodes of the communication chain. The method should reduce the number of aircraft required for mission execution without losing requirements for geometric route admissibility, communication stability, autonomy, and safety.

This objective is achieved by formalizing the selection problem, developing an algorithm-selection method, creating software tools for its implementation, conducting experimental studies and comparisons, and discussing the obtained results and directions for further research.

III. FORMALIZATION OF THE ALGORITHM SELECTION PROBLEM

This section presents a formalized problem statement, a model of the hazardous 3D environment, rules for adaptive algorithm selection, and UAV placement conditions for maintaining communications. The formal apparatus is used not as an independent theoretical construction but as a tool for unambiguous description of objects, constraints, and indicators: space, obstacles, route, relay positions, line of sight, communication range, risk, and the number of aircraft.

The logic of the section moves from the general environment model to a concrete decision-making procedure. First, the space, obstacles, route, and communication chain are defined; then the environmental features are introduced; after that the mechanism for multi-indicator assessment of algorithms is described; and the final methodological element is relay UAV placement and software implementation of this process.

A. FORMALIZED PROBLEM STATEMENT

A bounded three-dimensional space is considered, in which a route or communication chain must be formed between the initial and target mission points. To avoid ambiguity between the target point and time, time is denoted by t, the initial point by s, and the target point by g.

The state of the hazardous environment at time t is represented by the tuple

$$E(t) = \langle V, \Omega(t), H(x,t) \rangle, x \in V, \quad (1)$$

where V subset R^3 denotes the admissible mission volume; Ω (t) is the area occupied by obstacles at time t; and H(x,t) is the normalized value of the cyber-physical impact at point x of the workspace at time t. This notation shows that the environment is described not only by obstacle geometry but also by the distribution of impacts in 3D space.

The obstacle area is formed as the union of individual obstacles of arbitrary geometry:

$$\Omega(t) = o_1(t) \cup \ldots \cup o_m(t), o_j(t) \subset V, \quad (2)$$

where o_j(t) is the geometric area occupied by the j-th obstacle. The position, shape, and orientation of o_j(t) may change over time.

The UAV route is specified as an ordered sequence of points:

$$P = (p_0, p_1, \ldots, p_n), p_i \in V, p_0 = s, p_n = g, \quad (3)$$

where p_i is the i-th route point; s is the initial mission point; g is the target mission point; and n is the number of route segments.

The route is geometrically admissible if each segment does not intersect the obstacle area:

$$[p_i, p_{i+1}] \cap \Omega(t) = \emptyset, i = 0, \ldots, n-1. \quad (4)$$

In expression (4), [p_i,p_{i+1}] denotes the segment between neighboring route points. This condition is standard for motion-planning tasks and ensures the absence of collisions with obstacles.

To support communications, an ordered set of relay-aircraft positions is formed:

$$R = (r_1, r_2, \ldots, r_k), r_i \in V;$$
$$C_R = (s, r_1, \ldots, r_k, g), c_i = r_i (i = 1, \ldots, k) \quad (5)$$

where r_i is the position of the i-th relay aircraft and k is the number of aircraft in the communication chain.

The line-of-sight function between two positions is defined as

$$\mathrm{LOS}(c_i, c_{i+1}, t) = \begin{cases} 1 & \text{if } [c_i, c_{i+1}] \cap \Omega(t) = \emptyset \\ 0 & \text{otherwise} \end{cases}, \quad i = 0, \ldots, k \quad (6)$$

Neighboring aircraft in the communication chain must simultaneously satisfy the line-of-sight condition and the communication-range constraint:

$$\mathrm{LOS}(c_i, c_{i+1}, t) = 1, i = 0, \ldots, k,$$
$$\mathrm{d}(c_i, c_{i+1}) \le R_{\mathrm{eff}}(c_i, c_{i+1}, t) \quad (7)$$

where d(c_i,c_{i+1}) is the Euclidean distance between neighboring elements of chain C_R, and R_eff(c_i,c_{i+1},t) is the effective communication range between them considering the environment state.

It is reasonable to define the effective communication range through a degradation coefficient:

$$R_{\mathrm{eff}}(c_i, c_{i+1}, t) = R_0 \alpha_H([c_i, c_{i+1}], t), 0 \le \alpha_H \le 1б \quad (8)$$

where R_0 is the nominal communication range in the absence of impacts, and alpha_H is the degradation coefficient, which decreases under smoke, temperature effects, electromagnetic interference, cyberattacks, or other factors.

The task of algorithm selection and aircraft placement is formulated as minimization of the number of relay UAVs under geometric and communication constraints:

$$R^{\mathrm{opt}} = \underset{R \in R_{\mathrm{adm}}}{\operatorname{argmin}} |R|, \quad (9)$$

where R^opt is the optimal set of relay-aircraft positions within the adopted formulation; R_adm is the set of admissible placements satisfying the non-intersection, line-of-sight, and allowable-range conditions from (4), (6), and (7), as well as the mission requirements for safety, autonomy, and success.

In this formulation, the coordinate r_i=(x_i,y_i,z_i) describes the hovering or transit location of the i-th relay UAV, not its serial number or role in the swarm. If the mission is to create a flying LiFi/FSO network, each pair of neighboring positions must have an unblocked optical channel; if a radio network is used, the LOS condition can be replaced by a model of admissible signal level, interference, and losses. Thus, the algorithm-selection method is tied not to a specific physical transmitter type but to the class of constraints determining placement admissibility.

An illustrative example in 3D space can be represented as a scene with the initial point s, the target point g, several volumetric obstacles of arbitrary shape, a constructed route P, and a set of positions R for relay UAVs. In such an example it should be visible that the UAV route and the communication chain do not always coincide: the route may bypass an obstacle, whereas relays are placed so that visibility and allowable range between nodes are preserved.

The illustrative 3D example in Figures 1-4 shows how the proposed software represents the mission environment, route geometry, relay-UAV positions, and cyber-physical impacts. Yellow solid objects denote volumetric obstacles that block direct visibility and constrain route construction. Semi-transparent colored regions represent zones of physical or cyber-physical influence that may reduce the effective communication range or increase mission risk. Thin lines show route or communication-chain connections between UAV positions. The example demonstrates that the route followed by the UAVs and the communication chain used to maintain connectivity do not necessarily coincide: the route may bypass obstacles, whereas relay UAVs are placed so that visibility and admissible range between neighboring communication nodes are preserved.

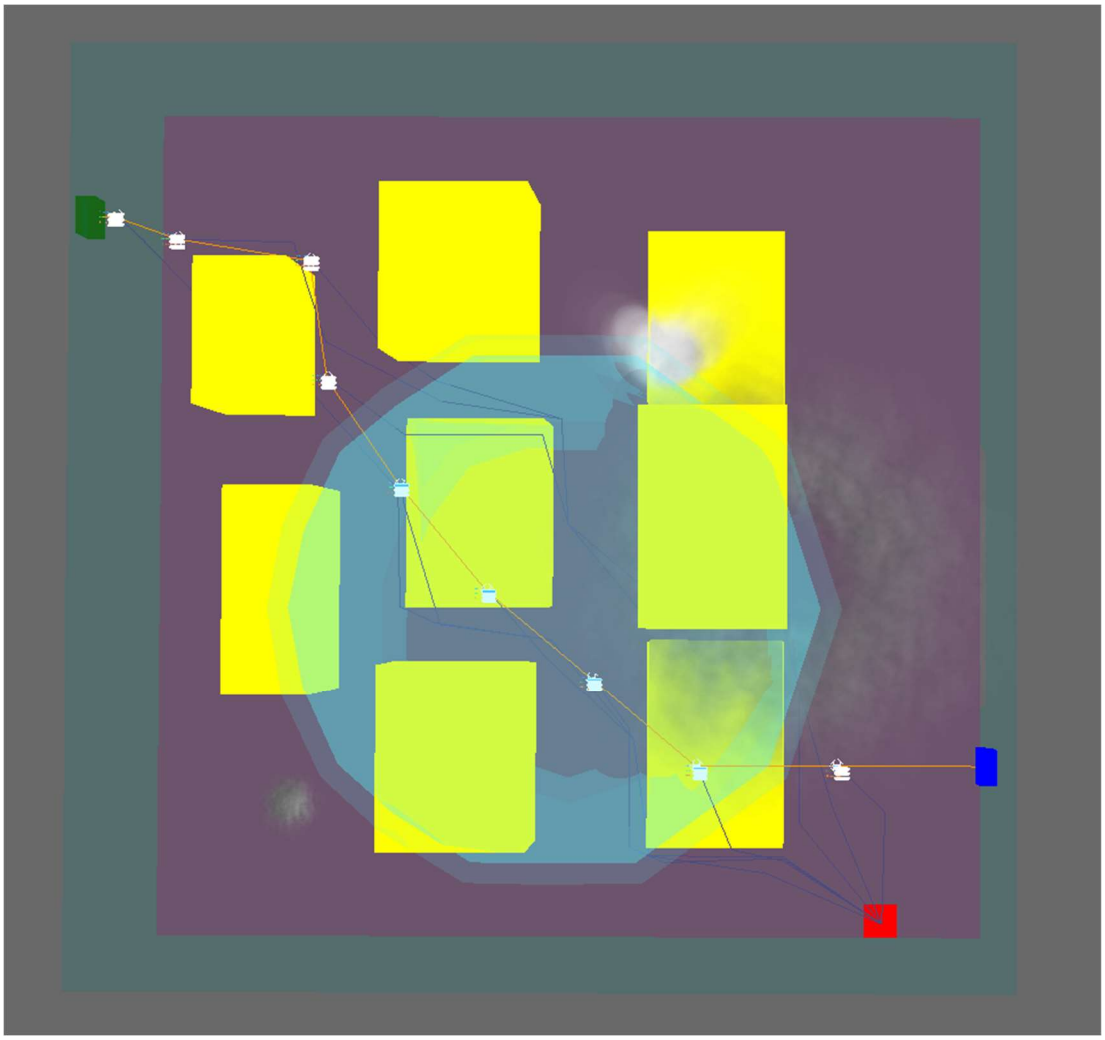

Figure 1. Top view of the simulated 3D environment showing volumetric obstacles, start and target areas, route geometry, and relay-UAV positions used to maintain the communication chain.

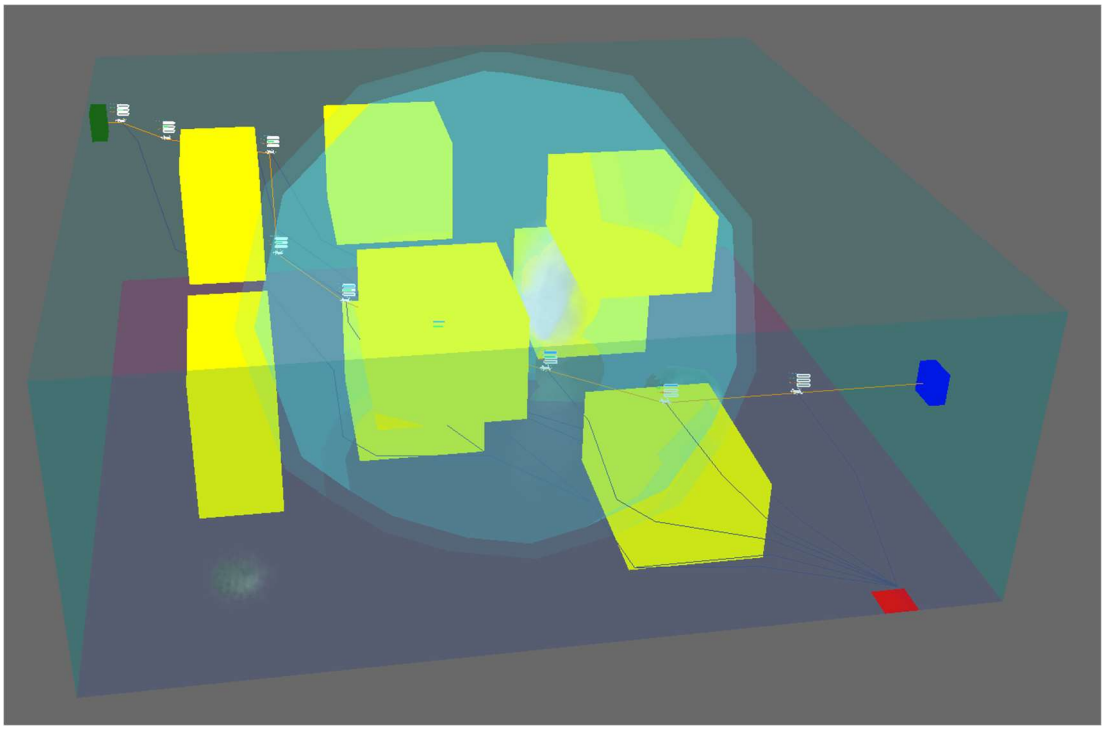

Figure 2. Isometric view of the same 3D scene showing the spatial relation between obstacles, cyber-physical impact zones, UAV positions, and communication links.

Figure 3. Local UAV state visualization showing cyber-impact, battery-level, and physical-impact indicators used for monitoring the condition of an individual UAV during mission execution.

Figure 4. Example of cyber-physical impact visualization in the 3D environment, where UAVs operate near obstacles and degraded-communication zones that affect route admissibility, risk, and communication stability.

IV. SELECTION METHOD

A. PRINCIPLE OF METHOD IMPROVEMENT

Known approaches to UAV routing often use one predefined algorithm, for example A*, RRT*, or greedy heuristic search. Such an approach is insufficient for a hazardous 3D space, because algorithm behavior substantially depends on obstacle density, obstacle-shape complexity, environment dynamics, communication constraints, and current cyber-physical risk.

The improvement consists in introducing a separate adaptive level for algorithm selection. It analyzes environment and mission parameters, forms a feature vector, and computes suitability estimates for the available algorithms. As a result, algorithm selection becomes dependent on real mission conditions rather than on a predefined scenario.

The comparative characteristics of the routing algorithms are summarized in Table 1, while the correspondence between task components and method implementation is summarized in Table 2.

Table 1. Comparative characteristics of routing algorithms for hazardous 3D space

Algorithm	Suitable application conditions	Advantages	Limitations for the UAV task
A*	The space is represented by a regular grid or graph; obstacle boundaries are correctly approximated by discretization	Determinism, clear heuristic, good route quality in regular grids	Dependence on discretization; increased costs in 3D; complexity in spaces with non-convex or fragmented obstacles
RRT*	Continuous space; obstacles of arbitrary, elongated, or fragmented shape; possible dynamic changes	Flexibility in space without a regular grid; ability to bypass complex obstacles	Randomness, need for smoothing, possible route-length increase
Greedy	Small occupied-volume fraction, no moving obstacles, priority of rapid admissible-solution generation	Low computational costs, fast response	Risk of local traps; weak robustness in dense or dynamic environments

Table 2. Correspondence between task components and implementation in the proposed method

Task component	Implementation in the proposed method
Arbitrary obstacle shape	Geometric checking of route-segment intersections with obstacles of arbitrary shape is used; shape complexity is included in the feature vector for algorithm selection.
Obstacle motion	Environment dynamics enters the dynamic_environment feature; significant changes trigger repeated assessment and replanning.
Cyber-physical impacts	The risk field H(x,t) is considered; it affects effective communication range, risk assessment, and the integral estimate of algorithms.
Communication support	After route construction, relay UAV placement is performed considering line of sight and communication range.
3D route formation	The selected algorithm builds a sequence of points in three-dimensional space considering environmental boundaries and obstacles.
Swarm-characteristic evaluation	The number of UAVs, route length, deployment time, communication stability, autonomy, and mission success are evaluated.
Reduction of aircraft number	The objective function (9) and the key efficiency indicator of UAV-number reduction relative to a baseline algorithm are used.

The general logic of the method can be represented as a sequential scheme in which each stage has input data, an action, and an expected result. This presentation shows that algorithm selection, route construction, and relay UAV placement are not isolated procedures.

The proposed method is modular. Each stage can be refined without destroying the overall logic. For example, the cyber-physical risk model can be specified as a single normalized coefficient in the interval [0,1] or detailed through separate components such as smoke, temperature, electromagnetic interference, and cyberattacks. Similarly, the set of algorithms may contain not only A*, RRT*, and greedy search, but also other approaches if a weight profile is defined for them.

Scheme 1 Sequence of stages of the proposed method

Stage	Input data	Action	Result
1. Environment and mission description	Space boundaries, obstacles, motion model, UAV, communication, and risk parameters	Formalize the current state of the cyber-physical environment	Scenario description suitable for algorithm assessment
2. Feature formation	Obstacle geometry, density, motion, communication channel, mission priority	Compress the full environment description into a normalized feature vector	Feature vector suitable for comparing alternatives
3. Algorithm selection	Normalized features and weight profiles for A*, RRT*, and greedy search	Compute integral algorithm estimates and select the best alternative	Primary algorithm and fallback option
4. Route construction	Selected algorithm, initial and target points, environment constraints	Find a geometrically admissible route or candidate chain of positions	Route checked for visibility, communication range, and risk
5. Swarm placement and evaluation	Route, communication parameters, autonomy and risk constraints	Place relay UAVs, remove redundant positions, and verify constraints	Number of UAVs, communication stability, autonomy reserve, admissible risk, and mission-success flag

B. ENVIRONMENT FEATURE VECTOR

For adaptive algorithm selection, the following feature vector is used:

$$F = \left(f_{\text{shape}}, f_{\text{density}}, f_{\text{dynamic}}, f_{\text{comm}}, f_{\text{cyber}}, f_{\text{priority}}\right)$$
$$f_j \in [0,1] \tag{10}$$

In expression (10), each feature is normalized to the interval [0,1], which ensures correct comparison of algorithms by several indicators without transforming the task into a separate optimization formulation.

The feature f_shape characterizes obstacle-shape complexity. It can be determined by the number of faces, curvilinearity, fragmentation, or another indicator of geometric complexity.

The feature f_density reflects obstacle density in the space:

$$f_{\text{density}} = \frac{\text{Vol}\left(\Omega(t)\right)}{\text{Vol}(V)} \tag{11}$$

In expression (11), Vol(Ω (t)) is the volume of the combined obstacle area defined in (2), and Vol(V) is the workspace volume. Using the volume of the union rather than the sum of individual obstacle volumes prevents double counting when objects overlap. If obstacles move, the value can be computed for the current time or averaged over a mission interval.

The feature f_dynamic describes the presence and intensity of moving obstacles or other dynamic changes in the environment. The feature f_comm specifies the level of communication constraints, including degradation of effective communication range, zones without line of sight, and channel-loss risk. The feature f_cyber characterizes cyber-physical risk associated with electromagnetic interference, smoke, temperature, chemical effects, cyberattacks, or combined impacts. The feature f_priority specifies the mission priority: speed, safety, minimum number of aircraft, or a balanced mode.

The features in vector (10) are not interchangeable. High obstacle density and high obstacle-shape complexity describe different environment properties: density indicates how much of the space is occupied by inaccessible regions, while shape complexity indicates how difficult it is for an algorithm to correctly bypass obstacle boundaries. The dynamics feature may consider obstacle speed, trajectory predictability, frequency of configuration changes, and the relative response time of the system. Communication and cyber-risk features can be specified as mission parameters in a simplified implementation or computed from measured or simulated channel quality and risk fields in an extended implementation.

Mission priority f_priority is introduced so that the same environment state can be processed differently depending on the goal. If speed is the priority, the selector can give greater weight to greedy or less expensive methods. If communication reliability is the priority, preference should shift toward algorithms forming routes with better visibility and lower channel-loss risk. If the priority is to minimize the number of aircraft, the assessment should more strongly consider route geometry and the possibility of removing redundant relay points.

Normalizing features to [0,1] is necessary but not sufficient. The source of values and measurement stability must also be controlled. If f_density is computed from a geometric model while f_comm is expert-defined, their accuracy and confidence differ. In practical implementation, it is useful to store not only feature values but also the way they were obtained: a configuration parameter, geometric-analysis result, telemetry measurement, or model forecast.

C. ASSESSMENT AND ALGORITHM SELECTION

Let the set of available algorithms be

$$A = \{A^*, \mathrm{RRT}^*, \mathrm{Greedy}\} \tag{12}$$

where A*, RRT*, and Greedy denote the A* algorithm, Rapidly-exploring Random Tree Star, and greedy search, respectively. The set can be extended, but three algorithms with different properties are sufficient to illustrate the method.

For each algorithm a in A, an integral suitability estimate is computed. To make estimates comparable even for different absolute weight values, weight normalization is performed first:

$$\tilde{w}_{a,j} = \frac{w_{a,j}}{W_a}, w_{a,j} \geq 0, \quad W_a = \sum_{l=1}^{q} w_{a,l} > 0 \tag{13}$$

where w_{a,j} is the initial weight of the j-th feature for algorithm a; q is the number of features in vector (10); and W_a is the sum of initial weights for algorithm a. If all initial weights for an algorithm are zero, a neutral profile w_tilde_{a,j}=1/q is used in practical implementation.

After normalization, the integral suitability estimate of an algorithm is defined as

$$S(a|F) = \sum_{j=1}^{q} \tilde{w}_{a,j} f_j \tag{14}$$

In expression (14), f_j is the normalized value of the j-th environment or mission feature, and S(a|F) is the integral suitability estimate of algorithm a for the current environment state. Under the conditions f_j in [0,1], w_tilde_{a,j}>=0, and sum w_tilde_{a,j}=1, the estimate S(a|F) also belongs to [0,1]. The weights are interpreted as an algorithm suitability profile rather than physical utility coefficients; therefore risk-related features are additionally controlled by separate threshold conditions introduced below.

The algorithm is selected by the rule

$$a^{\mathrm{opt}} = \underset{a \in A}{\mathrm{argmax}} S(a|F) \tag{15}$$

Equations (13)-(15) should be understood as a rule for ranking alternatives, not as a statement of global route optimality. They answer which algorithm should be launched for the current environment state. Route quality and the number of UAVs are evaluated after the selected algorithm has been executed.

If several algorithms have close estimates, a deterministic tie-break is applied according to safety priority, expected costs, or a predefined order. In addition, a second-ranked candidate algorithm is stored and can be used as a fallback if the primary algorithm fails to construct an admissible route.

For environments with arbitrary obstacle geometry, no regular grid, or dynamic changes, RRT* may be preferred. For environments already represented by a regular grid or graph, A* may be suitable. For scenarios with a small occupied-volume fraction, static obstacles, and priority of rapid admissible-solution generation, greedy search may be applied.

The adaptive-selection procedure can be represented as a flow of data and decisions separating feature collection, alternative assessment, fallback selection, and result recording.

Scheme 2. Algorithmic procedure of adaptive selection

Step	Action content	Purpose
1	Read mission parameters, space boundaries, initial and target points, UAV parameters, and basic communication constraints	Form the input task description
2	Compute geometric features: obstacle density, shape complexity, free-space availability, and visibility-loss zones	Evaluate obstacle form and density for algorithm selection

Step	Action content	Purpose
3	Compute dynamic and cyber-physical features: obstacle motion, impact intensity, channel-degradation risk	Consider temporal variability and environmental risk
4	Normalize features to a common scale and verify their source	Make heterogeneous features comparable
5	Compute feature contributions for each algorithm and store terms w_tilde_{a,j}f_j	Ensure explainability of the final estimate
6	Select the algorithm with the maximum estimate; apply a deterministic rule for close estimates	Obtain the primary and fallback algorithms
7	Construct a route using the selected algorithm; launch fallback in case of failure	Increase robustness to path-search failure
8	Place relay UAVs and minimize their number under line-of-sight and range constraints	Link the route with the communication chain
9	Evaluate UAV count, communication stability, deployment time, autonomy, risk, and success	Record data for comparison with baseline approaches

An important property of the procedure is explainability. In many autonomous-system tasks it is not enough to obtain a route; it is necessary to explain why this particular algorithm was selected. Therefore, the method stores feature values, weights, indicator contributions, and final estimates. This makes it possible after an experiment to verify whether algorithm selection followed the expected logic.

Another practical property is support for forced and auto modes. The forced mode is required for control experiments: it allows A*, RRT*, or Greedy to be launched explicitly under identical scenarios. The auto mode is used for the proposed method. Without this separation it is impossible to evaluate correctly whether adaptive selection provides an advantage over single-algorithm approaches.

In a dynamic environment, algorithm selection should not be a one-time action. If obstacle positions change after mission start, cyber-physical risk increases, or communication quality degrades, the system should reassess the feature vector. Replanning does not necessarily mean complete reconstruction of the entire route. If the change is limited to one local segment and does not destroy the communication chain, it is sufficient to locally modify the route segment or update several relay positions. However, if the environment changes significantly, repeated algorithm selection is justified.

The proposed procedure does not impose specific weight values. Weights can be expert-defined, calibrated from experiments, or tuned for a specific class of environments. For an initial implementation, an expert profile is sufficient: RRT* receives a higher weight for dynamics and risk, A* for environments represented by a grid or graph, and Greedy for speed priority and a small occupied-volume fraction. Further weight refinement should be based on experimental data.

D. UAV PLACEMENT FOR COMMUNICATION SUPPORT

Within the proposed approach, UAV placement is considered as the task of forming a communication chain based on the constructed route or directly within the admissible 3D space. After algorithm selection and route construction, the relay-aircraft placement stage is performed.

Initially, candidate positions may correspond to route points or space-discretization nodes. Then a minimization procedure removes intermediate positions if line of sight and admissible communication range are preserved between neighboring aircraft. This reduces the number of aircraft without violating communication connectivity.

The admissible placement conditions are

$$\begin{gathered} c_i \notin \Omega(t), c_{i+1} \notin \Omega(t), \\ \mathrm{LOS}(c_i, c_{i+1}, t) = 1, i = 0, \dots, k, \\ \mathrm{d}(c_i, c_{i+1}) \le R_{\mathrm{eff}}(c_i, c_{i+1}, t) \end{gathered} \tag{16}$$

In expression (16), the first two conditions prohibit placement of neighboring chain elements inside obstacles, the third ensures line of sight, and the fourth considers communication-range limits under cyber-physical impacts.

Thus, the routing and communication tasks are not solved in isolation. The routing algorithm affects route length, geometry, and visibility and therefore the number of relay aircraft. For obstacles of arbitrary shape, not only the fact of route-obstacle intersection but also the influence of obstacle shape on visibility is important. Two obstacles of equal volume may have different influence on the communication chain: a compact obstacle may block only a few directions, whereas an elongated or fragmented obstacle may block many potential communication lines.

Obstacle motion complicates the task further. If relay positions are selected only for the initial environment state, some visibility lines may be lost after a certain time. In such a situation, two mechanisms are needed: prediction of placement admissibility over a time interval and a replanning trigger. If trajectories are known, prediction may be simple; if motion has a random component, protective range reserves or avoidance of positions close to predicted obstacle-motion areas are advisable.

Optimization of the number of aircraft after route construction can be performed by a greedy procedure that removes intermediate points. If conditions (6) and (7) are preserved between two non-neighboring route points, the intermediate relays can be removed. Such a procedure does not guarantee a global optimum for all possible placements, but it is practical, fast, and well combined with different route-construction algorithms.

In hazardous space, aircraft placement also depends on safety constraints. Even if a point is suitable for communication, it may be undesirable due to high physical risk, a strong electromagnetic field, or the probability of control loss. Therefore, in an extended implementation, R_adm should include not only geometric and communication constraints but also risk constraints. This makes the task more complex but better corresponds to real conditions of swarm application.

Another practical aspect is the difference between placement for communication and the deployment route. A relay position can be communication-optimal but difficult to reach from a depot. In this article, the main emphasis is on algorithm selection and minimization of the number of aircraft; however, the proposed structure is compatible with further extension in which the delivery time of aircraft to positions and the autonomy balance between them are added to the assessment.

V. SOFTWARE IMPLEMENTATION OF THE METHOD

The method is implemented in a software system for modelling hazardous 3D space. The system uses Python, Panda3D, YAML configurations, CSV artifacts, InfluxDB, Grafana, and Docker. The simulation environment includes static and dynamic obstacles, moving objects with specified routes, and physical effects such as smoke, temperature, fog, smoke

contamination, electromagnetic interference, and cybernetic impacts.

The developed software system is a configurable three-dimensional simulation and experimental-validation environment for planning, deploying, and supervising relay-UAV communication chains between specified endpoints. Its Python/Panda3D client loads YAML-defined scenarios, represents static obstacles and predefined moving obstacles, constructs routes using A*, RRT*, or greedy search with optional weighted automatic selection, deploys and prunes relay UAVs, monitors battery and cyber-physical exposure, evaluates end-to-end communication quality, and records reproducible experimental metrics.

Three practical user profiles are supported: a simulation operator, who starts deployment and interacts with individual UAVs; a researcher or algorithm developer, who defines scenarios, selector weights, seeds, and launch modes and performs automated batch experiments; and an analyst or administrator, who examines CSV results and, when enabled, the InfluxDB/Grafana monitoring stack. These profiles describe usage workflows in the experimental prototype rather than software-enforced access-control roles.

The core client is executed locally with Python 3.12 and Panda3D 1.10.15 on a general-purpose workstation. YAML inputs and CSV outputs are sufficient for reproducible batch experiments; InfluxDB 2.7 and Grafana 12.2.1 are optional Docker services for time-series persistence and visualization. The implementation does not require distributed computing or dedicated UAV hardware. Its computational demand is determined mainly by scene complexity, route-search resolution, obstacle count, and the selected algorithm; local storage is required for application assets and experiment artifacts.

In the software implementation, adaptive algorithm selection is performed by the AlgorithmSelector component. It computes environment-factor values, feature contributions for each algorithm, and selects the algorithm with the highest estimate. The DronesPlaningManager component collects mission factors, calls the selector, records the selected algorithm in statistics, creates the corresponding search algorithm, and supports replanning in a dynamic environment.

The system configuration includes the auto mode, in which algorithm selection is performed adaptively, and forced launch modes for individual algorithms: a_star, rrt, and greedy. This makes it possible to compare the adaptive method with baseline single-algorithm approaches.

The system also records experimental indicators for each run. They include the selected algorithm, actual number of UAVs, deployment time, route length, average risk, physical impacts, communication stability, and mission-success flag.

VI. EVALUATION AND EXPERIMENTS

This section reports the experimental evaluation of the proposed method in the developed 3D simulation environment. The evaluation covers the complete workflow of a mission run: scenario loading, computation of environmental indicators, adaptive or forced algorithm selection, route construction, relay-UAV placement, and recording of run-level measurements. The adaptive mode is compared with forced single-algorithm modes under identical initial conditions.

The results are interpreted through two groups of indicators. The resource indicator is the number of UAVs required to maintain the route and communication chain. The guard indicators include route admissibility, deployment time, route length, communication stability, mission success, autonomy reserve, and cyber-physical risk. This structure makes it possible to report whether the adaptive method changes UAV count and, at the same time, whether mission quality and safety constraints are preserved. The numerical outcomes of the 100-run experimental series are presented in Section VI.B.

A. METRICS FOR EVALUATING SWARM CHARACTERISTICS

The evaluation metrics are calculated after algorithm selection, route construction, and relay UAV placement. They make it possible to analyze the resource cost of a mission together with the constraints that determine whether the obtained solution is admissible. Therefore, the number of UAVs is analyzed together with route length, deployment time, communication-chain stability, mission success, autonomy reserve, and integral cyber-physical risk.

The relative change in the number of UAVs compared with a baseline algorithm is computed as:

$$\Delta_N = \frac{N_{\text{base}} - N_{\text{adapt}}}{N_{\text{base}}} \times 100\%, N_{\text{base}} > 0 \quad (17)$$

where N_base is the number of aircraft obtained for a fixed baseline algorithm, N_adapt is the number of aircraft obtained for the adaptive method, and Delta_N>0 means a reduction in the number of aircraft.

UAV-number reduction is evaluated only together with guard metrics. The following notation is introduced: MS is mission success, CS is communication-chain stability, AR is autonomy reserve, and Risk is integral cyber-physical risk. The adapt index corresponds to the adaptive method, the base index to the baseline single-algorithm approach, and C_min, A_min, and Risk_max to admissible threshold values.

$$\text{MS}_{\text{adapt}} \geq \text{MS}_{\text{base}} \quad (18)$$

Mission success for the adaptive method must not be lower than mission success for the baseline approach.

$$\text{CS}_{\text{adapt}} \geq C_{\min} \quad (19)$$

Communication-chain stability must remain no lower than the minimum acceptable level.

$$\text{AR}_{\text{adapt}} \geq A_{\min} \quad (20)$$

Autonomy reserve after the actions have been performed must not be lower than the admissible threshold.

$$\text{Risk}_{\text{adapt}} \leq \text{Risk}_{\max} \quad (21)$$

Integral cyber-physical risk must not exceed the specified limit.

To explain the numerical assessment of communication stability in experimental runs, the separate CS_run indicator is used. In the current software implementation it is a normalized engineering metric based on telemetry of a single run, not a complete physical radio-channel model:

$$\mathrm{CS}_{\mathrm{run}} = \min(1, \max(0, 1 - 0.5\bar{R}_{\mathrm{cyber}} - 0.3\bar{I}_{\mathrm{phys}})) \quad (22)$$

In (22), Rbar_cyber is the average avg_cyber_risk value in the time measurements of the run; Ibar_phys is the average avg_physical_effect_intensity value after normalization or clipping to a non-negative scale. The coefficients 0.5 and 0.3 are the current penalty weights in the experiment logger. The min and max operations explicitly restrict CS_run to [0,1].

The uav_count metric is central, but it cannot be considered in isolation. Reducing the number of aircraft is meaningful only when the route remains admissible and the communication chain does not lose stability. The path_distance metric helps distinguish reduction due to a shorter route from reduction due to better visibility geometry for a similar route length. The deploy_time metric reflects practical suitability. The communication_stability metric should consider both geometric connectivity and channel quality. The autonomy_reserve metric is important to prevent overloading individual aircraft. The Risk metric summarizes the influence of the hazardous environment on mission execution, for example as the average or maximum H(x,t) along the route and at relay positions.

Thus, evaluation must be multidimensional. The main target indicator is reduction in the number of UAVs, but the conclusion about method effectiveness is made only after checking that other critical characteristics are not degraded. This approach corresponds to the engineering logic of systems with limited resources: one resource is optimized under constraints on quality and safety.

B. RESULTS OF EXPERIMENTAL COMPARISON

The developed software environment was already capable of representing dynamic elements, including predefined moving 3D obstacles, time-windowed cyber-physical influence zones, continuously changing UAV states, and online route monitoring and replanning. Nevertheless, the controlled comparison reported in this subsection comprised 100 runs over five fixed 3D layouts. For this validation matrix, obstacle motion was disabled and each layout was treated as a reproducible snapshot of the broader dynamic-capable environment. Five fixed pseudorandom seeds and four algorithmic modes were used; the seeds reproduced stochastic elements of scenario generation and algorithm execution and were not treated as independent experimental samples.

The experimental comparison included 100 runs: five static 3D-environment scenarios, five fixed pseudorandom generator seeds, and four compared algorithmic variants. The seeds were used only to reproduce stochastic elements of scenario generation and algorithm execution; they were not treated as experimental random samples.

The scenarios included a gate corridor, a dense block-obstacle cluster, a zigzag maze, a layered altitude configuration, and a space with degraded electromagnetic conditions. For each scenario, the occupied-volume fraction, communication constraint, and obstacle-shape complexity were specified; these parameters were used as input conditions for comparing launch modes.

For each scenario, four modes shown in Table 3 were launched. Each mode was repeated five times with the same set of seeds; therefore, the total number of runs was 5 scenarios * 4 modes * 5 repetitions = 100.

Table 3. Launch modes used in the experimental series

Approach	Description
a_star	Forced use of A*.
rrt	Forced use of RRT*.
greedy	Forced use of the greedy algorithm.
auto	Proposed adaptive algorithm selection.

In all 100 runs, the mission was completed successfully, meaning that success_rate equalled 1 for each mode. Because the reported validation used fixed layouts, the dynamics feature did not distinguish the tested cases, and the adaptive auto mode selected a_star in all 25 adaptive runs. This 25/25 result is consistent with the selector settings and the scenario density and shape-complexity values. It confirms reproducible selector operation for the fixed-snapshot matrix, but it does not demonstrate algorithm switching or replanning in response to obstacles moving during a mission.

Aggregated results by launch modes are presented in Table 4. The values were obtained by aggregating the results of separate runs for each mode.

Table 4. Aggregated results of the experimental series by launch modes

Mode	Runs	N_UAV, mean	deploy_time, s	path_distance	CS, mean	success
a_star	25	9.4 +/- 0.8165	8.9011 +/- 0.4959	58.1088 +/- 6.0414	0.6283 +/- 0.074	1
auto	25	9.4 +/- 0.8165	8.9010 +/- 0.5007	58.1088 +/- 6.0414	0.6283 +/- 0.074	1
greedy	25	9.4 +/- 0.8165	8.9011 +/- 0.5015	58.1088 +/- 6.0414	0.6283 +/- 0.074	1
rrt	25	9.4 +/- 0.8165	10.4252 +/- 3.6488	58.1088 +/- 6.0414	0.6279 +/- 0.0728	1

All four modes produced a mean of 9.4 relay UAVs, and Delta_N was zero for every matched auto-baseline comparison. The difference in standard deviation arose from scenario complexity rather than from the algorithm: scenario v3_zigzag_maze required 11 aircraft, whereas the other scenarios required 9. This is a null result for the target resource indicator and therefore does not support a claim that the adaptive mode reduced the relay count in the tested matrix.

The null result is consistent with a scenario-specific geometric and communication floor. All compared pathfinders use the same final pruning procedure, which retains the farthest collision-free waypoint within the adopted visibility range. An intermediate relay is removed only when the resulting neighboring nodes preserve line of sight, satisfy the effective-range limit, and maintain end-to-end connectivity. After this pruning, four scenarios required nine relays; the zigzag-maze scenario required eleven because additional route turns and obstacle-induced visibility breaks divided the route into more feasible link segments. No further relay could be removed by the implemented procedure without violating at least one constraint. These values are minimum sufficient counts for the adopted routes and placement procedure, not proof of a global minimum over all possible continuous 3D placements.

By the average number of UAVs, all modes produced the same result: 9.4 aircraft on average over all scenarios. The difference in standard deviation was caused not by the

algorithm but by scenario complexity: scenario v3_zigzag_maze required 11 aircraft, whereas the other scenarios required 9. Thus, in the conducted static series, reduction of the number of UAVs by the adaptive mode was not recorded.

This result can be explained by the geometric and communication constraints of the tested environments. For the given mission volume, obstacle configuration, and effective communication range, the relay-placement procedure produced the same minimum sufficient communication chain for all compared modes. In the four less restrictive scenarios, nine UAVs were sufficient to preserve line of sight, admissible range, and route-chain connectivity. In the zigzag-maze scenario, eleven UAVs were required because additional route turns and obstacle-induced visibility breaks increased the number of necessary relay positions. Therefore, the absence of UAV-count reduction in this experimental series indicates that the tested scenarios were already close to the feasible lower bound defined by the adopted placement procedure and constraints, rather than that the adaptive selector was ineffective.

By deployment time, auto practically coincided with a_star and greedy because A* was selected in all adaptive runs. Compared with rrt, the adaptive mode had a smaller mean deploy_time: 8.9010 s versus 10.4252 s. At the same time, RRT* produced a smaller mean time in scenarios v4_layered_altitude and v5_em_degraded_sparse; therefore, this result should not be interpreted as a universal advantage of auto over RRT*.

Table 5 presents adaptive results by the v1-v5 scenarios described above. The lower CS value for v5 is caused by communication_constraint=0.82 and related physical impacts, not by algorithm selection.

Table 5. Results of adaptive auto mode by scenarios

Scenario	density	comm.	shape	alg.	N_UAV	deploy_time, s	CS
v1	0.48	0.42	0.62	a_star	9	9.6942	0.7306
v2	0.66	0.50	0.74	a_star	9	8.5016	0.6700
v3	0.58	0.55	0.80	a_star	11	9.2611	0.5810
v4	0.52	0.48	0.88	a_star	9	8.5187	0.6400
v5	0.36	0.82	0.54	a_star	9	8.5292	0.5200

Comparison of the adaptive mode with baseline modes showed that the difference in the number of UAVs was 0 for all considered pairs of scenarios and baseline algorithms. The difference in geometric-route length was also 0, indicating the same route length within the current formulation. For the total length of UAV routes, the adaptive mode was on average shorter than greedy heuristic search by 1.0859, almost coincided with A*, and had mixed results compared with RRT*. The absolute difference in communication stability between adaptive and baseline modes did not exceed 0.0037.

Accordingly, the demonstrated value of this series is narrower: the adaptive pipeline preserved a feasible communication chain and did not increase relay demand relative to the baselines under matched conditions. A positive relay-count reduction must be tested in scenarios where the candidate algorithms produce meaningfully different detours or visibility geometries that lie above the same feasibility floor.

Thus, the conducted experimental series confirmed the operability of the multi-indicator selection mechanism, reproducibility of metric collection, and absence of degradation in guard characteristics in the tested static scenarios. At the same time, this series is not sufficient for a statistically confirmed statement about reducing the number of UAVs, because auto did not differ from a_star by the number of aircraft and selected the same algorithm in all adaptive runs. The results should therefore be interpreted within the considered static scenarios.

VII. DISCUSSION

The proposed method eliminates the main limitation of fixed algorithm selection: one algorithm cannot be equally effective for all classes of hazardous 3D environments. A* is appropriate when the space is represented by a regular grid or graph; RRT* is appropriate when obstacles have arbitrary geometry or the environment changes over time; greedy search is appropriate when the occupied-volume fraction is small, obstacles are static, and the priority is rapid generation of an admissible solution. The adaptive selector makes it possible to change the algorithm depending on mission conditions.

A principal property of the proposed approach is the connection between algorithm selection and environment characteristics: arbitrary obstacle shape, obstacle motion, and cyber-physical impacts. In addition, the method is not limited to route construction; it includes the stage of UAV placement for maintaining the communication chain, which allows direct evaluation and minimization of the number of aircraft.

A limitation of the current implementation is that some cyber-physical parameters are provided to the selector as an aggregated risk or mission parameter. Therefore, conclusions regarding the influence of cyber-physical factors concern this aggregated formulation rather than a complete telemetry model of the environment.

The proposed approach has practical value because it allows one software loop to be used for different types of hazardous spaces. If the occupied-volume fraction increases, moving obstacles appear, or communication conditions degrade, the algorithm does not have to be changed manually: the system performs selection and records its explanation in the report.

The method allows algorithms to be compared not only by route length. In classical motion-planning tasks, a shorter route is often considered better; however, in the communication-chain task, the route must also be evaluated through the number of relays, visibility between them, communication stability, and risk. Therefore, adaptive selection creates a bridge between geometric optimality and swarm resource efficiency.

The main threat to validity is the limited scenario matrix. The simulator already represents dynamic elements and supports online monitoring and replanning, but the reported 100-run validation used fixed layouts; therefore, the adaptive selector consistently selected A*. This outcome is correct for the tested settings but cannot be generalized to moving obstacles, abrupt risk changes, or channel degradation during a mission. The applicability limits of the method are also determined by feature quality and the set of available algorithms: if all available algorithms perform poorly in a particular environment class, the selection mechanism itself cannot produce a high-quality route.

VIII. CONCLUSIONS

The main contribution of the study is the proposed and experimentally tested method for adaptive selection of algorithms that considers cyber-physical environment parameters and supports requirements for placement, communication, and route-search characteristics in hazardous 3D space during UAV missions. The method considers arbitrary obstacle shape, obstacle motion, communication constraints, and cyber-physical impact parameters through a normalized environment-feature vector.

Unlike known single-algorithm approaches, the proposed method compares A*, RRT*, and greedy search by several indicators, supports fallback and replanning, and links route construction with relay UAV placement. This creates a basis for evaluating swarm characteristics and reducing the number of aircraft required for mission execution.

The conducted experimental series confirmed the operability of the adaptive-selection software loop and metric collection: 100 runs were completed, all missions were successful, and controlled safety and communication characteristics did not degrade. Within the considered static scenarios, a reduction in the number of UAVs was not recorded; this limits the interpretation of the experiment and shows that, for the given set of conditions, the main confirmed effect is correct adaptive selection without degradation of mission constraints.

This result should be interpreted in the context of the tested environment size and communication constraints. In most scenarios, the implemented placement procedure produced nine relay UAVs, while the zigzag-maze scenario required eleven because of additional visibility breaks and route turns. These are the minimum sufficient counts returned by the implemented placement procedure under the adopted line-of-sight, effective-range, and connectivity constraints; they do not establish a global continuous-space optimum. The zero reduction therefore reflects a scenario-specific, constraint-conditioned floor shared by the compared solutions. It neither demonstrates relay-count superiority nor indicates a failure of the selector.

As a priority, future validation will use genuinely dynamic scenarios in which obstacles move during mission execution and the feature vector is recomputed over time. Adaptive and forced modes will be compared under matched obstacle trajectories and seeds, with algorithm transitions, replanning success and latency, communication-chain continuity, safety constraints, and relay count reported explicitly. These experiments are required before conclusions about selector performance in dynamic environments can be made.

This result should be interpreted in the context of the tested environment size and communication constraints. In most scenarios, the implemented placement procedure produced nine relay UAVs, while the zigzag-maze scenario required eleven relay UAVs because of additional visibility breaks and route turns. These values can be considered the minimum sufficient UAV numbers obtained by the implemented placement procedure under the adopted line-of-sight, effective-range, and connectivity constraints. Therefore, the absence of UAV-count reduction does not indicate failure of the adaptive selector. It shows that, for the tested scenarios, the relay chain was already constrained by environment geometry and communication requirements, and further reduction would likely violate visibility, range, or connectivity conditions.

Further research may address situations in which the mission objective can repeatedly change during execution by an individual UAV or a swarm, as well as conditions involving failures of individual aircraft. This may require neural-network or other tools for dynamic modification of the placement plan or route. Another promising task concerns heterogeneous mobile systems that combine individual aircraft or/and ground vehicles and platforms capable of delivering several aircraft to a corresponding point in space for providing humanitarian demining, active counter missions [36, 37] and technical inspection of critical objects [38].

References

[1] L. Yu. Ostapenko, V. S. Kharchenko, "Algorithms for route formation in 2D/3D space using mobile means to provide communications under destruction conditions," *Measuring and Computing Devices in Technological Processes*, no. 2, pp. 168-178, 2024. https://doi.org/10.31891/2219-9365-2024-78-20. (in Ukrainian)

[2] L. Yu. Ostapenko, V. S. Kharchenko, "System for modelling obstacle overcoming and communication organization in hazardous spaces: structure and experimental studies," *Control, Navigation and Communication Systems*, no. 3(81), pp. 128-135, 2025. https://doi.org/10.26906/SUNZ.2025.3.128. (in Ukrainian).

[3] K. Leichenko, H. Fesenko, V. Kharchenko, O. Illiashenko, "Deployment of a UAV swarm-based LiFi network in the obstacle-ridden environment: algorithms of finding the path for UAV placement," *Radioelectronic and Computer Systems*, no. 1, pp. 176-195, 2024. https://doi.org/10.32620/reks.2024.1.14.

[4] H. Fesenko, O. Illiashenko, V. Kharchenko, K. Leichenko, A. Sachenko, L. Scislo, "Methods and software tools for reliable operation of flying LiFi networks in destruction conditions," *Sensors*, vol. 24, no. 17, Article 5707, 2024. https://doi.org/10.3390/s24175707.

[5] L. Gupta, R. Jain, G. Vaszkun, "Survey of important issues in UAV communication networks," *IEEE Communications Surveys & Tutorials*, vol. 18, no. 2, pp. 1123-1152, 2016. https://doi.org/10.1109/COMST.2015.2495297.

[6] Y. Zeng, R. Zhang, T. J. Lim, "Wireless communications with unmanned aerial vehicles: opportunities and challenges," *IEEE Communications Magazine*, vol. 54, no. 5, pp. 36-42, 2016. https://doi.org/10.1109/MCOM.2016.7470933.

[7] M. Mozaffari, W. Saad, M. Bennis, Y.-H. Nam, M. Debbah, "A tutorial on UAVs for wireless networks: applications, challenges, and open problems," *IEEE Communications Surveys & Tutorials*, vol. 21, no. 3, pp. 2334-2360, 2019. https://doi.org/10.1109/COMST.2019.2902862.

[8] I. Bekmezci, O. K. Sahingoz, S. Temel, "Flying ad-hoc networks (FANETs): a survey," *Ad Hoc Networks*, vol. 11, no. 3, pp. 1254-1270, 2013. https://doi.org/10.1016/j.adhoc.2012.12.004.

[9] O. S. Oubbati, M. Atiquzzaman, P. Lorenz, M. H. Tareque, M. S. Hossain, "Routing in flying ad hoc networks: Survey, constraints, and future challenge perspectives," *IEEE Access*, vol. 7., pp. 81057-81105, 2019. https://doi.org/10.1109/ACCESS.2019.2923840.

[10] H. Rodrigues, A. Coelho, M. Ricardo, R. Campos, "Joint energy and performance aware relay positioning in flying networks," *IEEE Access*, vol. 10, pp. 50875-50890, 2022. https://doi.org/10.1109/ACCESS.2022.3168695.

[11] N. E.-D. Safwat, I. M. Hafez, F. Newagy, "3D placement of a new tethered UAV to UAV relay system for coverage maximization," *Electronics*, vol. 11, no. 3, article 385, 2022. https://doi.org/10.3390/electronics11030385.

[12] X. Wang, L. Fu, N. Cheng, R. Sun, T. Luan, W. Quan, K. Aldubaikhy, "Joint flying relay location and routing optimization for 6G UAV-IoT networks: a graph neural network-based approach," *Remote Sensing*, vol. 14, no. 17, Article 4377, 2022. https://doi.org/10.3390/rs14174377.

[13] H. Goehar, A. S. Khwaja, A. A. Alnoman, A. Anpalagan, M. Jaseemuddin, "Investigation of a HAP-UAV collaboration scheme for throughput maximization via joint user association and 3D UAV placement," *Sensors*, vol. 23, no. 13, Article 6095, 2023. https://doi.org/10.3390/s23136095.

[14] A. Humayed, J. Lin, F. Li, B. Luo, "Cyber-physical systems security: A survey," *IEEE Internet of Things Journal*, vol. 4, no. 6, pp. 1802-1831. https://doi.org/10.1109/JIOT.2017.2703172.

[15] C. Rani, H. Modares, R. Sriram, D. Mikulski, F. L. Lewis, "Security of unmanned aerial vehicle systems against cyber-physical attacks," *The Journal of Defense Modeling and Simulation*, vol. 13, no. 3, pp. 331-342, 2016. https://doi.org/10.1177/1548512915617252.

[16] E. W. Dijkstra, "A note on two problems in connexion with graphs," *Numerische Mathematik*, vol. 1, no. 1, pp. 269-271, 1959. https://doi.org/10.1007/BF01386390.
[17] P. E. Hart, N. J. Nilsson, B. Raphael, "A formal basis for the heuristic determination of minimum cost paths," *IEEE Transactions on Systems Science and Cybernetics*, vol. 4, no. 2, pp. 100-107, 1968. https://doi.org/10.1109/TSSC.1968.300136.
[18] S. M. LaValle, J. J. Kuffner, "Randomized kinodynamic planning," *The International Journal of Robotics Research*, vol. 20, no. 5, pp. 378-400, 2001. https://doi.org/10.1177/02783640122067453.
[19] J. J. Kuffner, S. M. LaValle, "RRT-Connect: an efficient approach to single-query path planning," *Proceedings of the 2000 IEEE International Conference on Robotics and Automation (2000 ICRA)*, San Francisco, CA, USA, 24-28 April 2000, vol. 2, pp. 995-1001. https://doi.org/10.1109/ROBOT.2000.844730.
[20] S. Karaman, E. Frazzoli, "Sampling-based algorithms for optimal motion planning," *The International Journal of Robotics Research*, vol. 30, no. 7, pp. 846-894, 2011. https://doi.org/10.1177/0278364911406761.
[21] G. Aiello, K. P. Valavanis, A. Rizzo, "Fixed-wing UAV energy efficient 3D path planning in cluttered environments," *Journal of Intelligent & Robotic Systems*, vol. 105, Article 60, 2022. https://doi.org/10.1007/s10846-022-01608-1.
[22] L. Cao, L. Wang, Y. Liu, S. Yan, "3D trajectory planning based on the rapidly-exploring random tree-connect and artificial potential fields method for unmanned aerial vehicles," *International Journal of Advanced Robotic Systems*, vol. 19, no. 5, 2022. https://doi.org/10.1177/17298806221118867.
[23] M. Hooshyar, Y.-M. Huang, "Meta-heuristic algorithms in UAV path planning optimization: a systematic review (2018-2022)," *Drones*, vol. 7, no. 12, Article 687, 2023. https://doi.org/10.3390/drones7120687.
[24] T. M. Cabreira, L. B. Brisolara, P. R. Ferreira Jr., "Survey on coverage path planning with unmanned aerial vehicles," *Drones*, vol. 3, no. 1, Article 4, 2019. https://doi.org/10.3390/drones3010004.
[25] L. Yang, J. Qi, D. Song, J. Xiao, J. Han, Y. Xia, "Survey of robot 3D path planning algorithms," *Journal of Control Science and Engineering*, vol. 2016, Article ID 7426913, 2016. https://doi.org/10.1155/2016/7426913.
[26] T. L. Saaty, "A scaling method for priorities in hierarchical structures," *Journal of Mathematical Psychology*, vol. 15, no. 3, pp. 234-281, 1977. https://doi.org/10.1016/0022-2496(77)90033-5.
[27] C.-T. Chen, "Extensions of the TOPSIS for group decision-making under fuzzy environment," *Fuzzy Sets and Systems*, vol. 114, no. 1, pp. 1-9, 2000. https://doi.org/10.1016/S0165-0114(97)00377-1.
[28] A. Mardani, A. Jusoh, K. M. D. Nor, Z. Khalifah, N. Zakwan, A. Valipour, "Multiple criteria decision-making techniques and their applications: A review of the literature from 2000 to 2014," *Economic Research-Ekonomska Istraživanja*, vol. 28, no. 1, pp. 516-571, 2015. https://doi.org/10.1080/1331677X.2015.1075139.
[29] A. Kumar, B. Sah, A. R. Singh, Y. Deng, X. He, P. Kumar, R. C. Bansal, "A review of multi criteria decision making (MCDM) towards sustainable renewable energy development," *Renewable and Sustainable Energy Reviews*, vol. 69, pp. 596-609, 2017. https://doi.org/10.1016/j.rser.2016.11.191.
[30] D. Jato-Espino, E. Castillo-Lopez, J. Rodriguez-Hernandez, J. C. Canteras-Jordana, "A review of application of multi-criteria decision making methods in construction," *Automation in Construction*, vol. 45, pp. 151-162, 2014. https://doi.org/10.1016/j.autcon.2014.05.013.
[31] N. I. Sarkar, S. Gul, "Artificial intelligence-based autonomous UAV networks: A survey," *Drones*, vol. 7, no. 5, Article 322, 2023. https://doi.org/10.3390/drones7050322.
[32] T. R. Beegum, M. Y. I. Idris, M. N. Ayub, H. A. Shehadeh, "Optimized routing of UAVs using bio-inspired algorithm in FANET: A systematic review," *IEEE Access*, vol. 11, pp. 15588-15622, 2023. https://doi.org/10.1109/ACCESS.2023.3244067.
[33] M. Hosseinzadeh, F. M. Husari, M. S. Yousefpoor, J. Lansky, H. Min, "A local filtering-based energy-aware routing scheme in flying ad hoc networks," *Scientific Reports*, vol. 14, Article 17733, 2024. https://doi.org/10.1038/s41598-024-68471-y.
[34] M. K. Banafaa, O. Pepeoglu, I. Shayea, A. Alhammadi, Z. A. Shamsan, M. A. Razaz, M. Alsagabi, S. A. Al-Sowayan, "A comprehensive survey on 5G-and-beyond networks with UAVs: applications, emerging technologies, regulatory aspects, research trends and challenges," *IEEE Access*, vol. 12, pp. 7786-7826, 2024. https://doi.org/10.1109/ACCESS.2023.3349208.
[35] M. C. Mayarakaca, B. M. Lee, "A survey on non-orthogonal multiple access for unmanned aerial vehicle networks: machine learning approach," *IEEE Access*, vol. 12, pp. 51138-51165, 2024. https://doi.org/10.1109/ACCESS.2024.3385860.
[36] Y. Zheng, G. Shcherbakova, B. Rusyn, A. Sachenko, N. Volkova, I. Kliushnikov, S. Antoshchuk, "Wavelet transform cluster analysis of UAV images for sustainable development of smart regions due to inspecting transport infrastructure," *Sustainability*, vol. 17, issue 3, 927, 2025. https://doi.org/10.3390/su17030927.
[37] O. Fedorovich, O. Prokhorov, D. Krytskyi, O. Malyeyeva, O. Leshchenko, R. Trishch, "Modeling of an attack mission by strike drones under active enemy counteraction," *Radioelectronic and Computer Systems*, vol. 1, pp. 34-52, 2026. https://doi.org/10.32620/reks.2026.1.03.
[38] O. Zastavnyy, L. Dubchak, V. Kochan, O. Savenko, Z. Bernas, N. Vasylkiv, "Integrated hardware–software complex for wind turbine blade defect classification," *Radioelectronic and Computer Systems*, vol. 1, pp. 111-124, 2026. https://doi.org/10.32620/reks.2026.1.08.

***LEONID OSTAPENKO** graduated Kharkiv National University of Radio Electronics (2012), Master's Degree in "Software and Multimedia Analyst". PhD student of the Department of Cybersecurity and Intelligent Information Technologies, National Aerospace University "KhAI", Kharkiv, Ukraine. Scientific interests: UAVs, Software engineering and modeling, Simulation systems for application of UAVs and UAV swarms in dangerous spaces.*

***Prof. VYACHESLAV KHARCHENKO**, graduated Kharkiv Higher Military Engineering College of Rocket Troops, Dr. of Sciences in Engineering (1995), Corr. Member of National Academy of Science of Ukraine (2025). Head of the Department of Cybersecurity and Intelligent Information Technologies, National Aerospace University "KhAI", Kharkiv, Ukraine. Scientific interests: Dependable intelligent computing; Resilience, safety and cybersecurity of I&C systems and critical infrastructures; AI-UXV systems for dangerous spaces; AI powered applications; AI vs AI scenarios and game modelling.*